A Monte Carlo study of titrating polyelectrolytes

Magnus Ullner[a] and Bo Jönsson[b]
Physical Chemistry 2, Chemical Center, University of Lund, P.O. Box 124, S-221 00 Lund, Sweden

Bo Söderberg[c] and Carsten Peterson[d]
Department of Theoretical Physics, University of Lund, Sölvegatan 14A, S-223 62 Lund, Sweden

(Received 20 December 1994; accepted 9 November 1995)

Monte Carlo simulations have been used to study three different models for linear, titrating polyelectrolytes in a salt-free environment: (i) a rigid polymer with rigid bonds (rigid rod); (ii) a flexible polymer with rigid bonds; and (iii) a flexible polymer with flexible bonds. The use of a very efficient pivot algorithm has made it possible to simulate very long chains, with up to several thousand titrating groups. The results have been compared to a mean field approximation for a rigid rod and variational results emanating from a Flory type approach. It is found that the rigid rod mean field model gives a qualitatively correct description for the apparent dissociation constant for all three models. At room temperature, the energy contribution to the apparent dissociation constant often dominates over the entropic term, which partly explains the relative success of this approach. In the case of flexible bonds, both the conformational behavior and the behavior of the apparent dissociation constant are well described by a variational ansatz with a quadratic term, largely thanks to the harmonicity of the bonds themselves. The approach is less successful for rigid bonds, which becomes evident for highly charged chains where a harmonic entropy term is incorrect. This can be remedied by replacing it with an expression valid in the strong coupling regime. Empirical scaling expressions have also been found, primarily for the end-to-end distance. © *1996 American Institute of Physics.* [S0021-9606(96)50607-3]

I. INTRODUCTION

The term polyelectrolyte is sometimes used to cover a very wide field including all types of charged macromolecules, i.e., proteins, synthetic colloids, membranes as well as flexible polymers with charged groups. Here, we will concentrate on the latter category and in particular polymers with titrating groups, so-called weak polyelectrolytes, where the amount of charge will vary with the solution pH.

Real polyelectrolytes can sometimes show a quite complex titration behavior involving abrupt conformational changes at a given degree of ionization. The helix-coil transformation of, for example, poly-*L*-glutamic acid is an illustrative example.[1] Other polyelectrolytes like polyacrylic acid[2] or hyaluronic acid[3] show a monotonic increase of the apparent dissociation constant at increased ionization. Obviously, the electrostatic interactions play a major role in the solution behavior of polyelectrolytes, for example, the presence of charge makes further ionization of the polymer more difficult and biases the conformations towards more extended structures.

In the Monte Carlo simulations presented here, focus will be on the electrostatic interactions and on how they affect conformational and energetic properties of a weak polyelectrolyte. A real polyelectrolyte solution will always contain a certain amount of neutral salt as well as a finite polymer concentration, both of which will act to screen the monomer–monomer Coulomb interaction. We will simplify the problem by neglecting the screening caused by added salt and finite polymer concentration. This is of course a drastic simplification, but it will on the other hand, allow us to investigate polymers with a significantly larger number of monomers and also to more clearly identify long range electrostatic effects. The disadvantage is of course that comparisons with experiments become difficult. However, the unscreened Coulomb chain represents a limiting case of considerable interest.[4]

Titrating polyelectrolytes have recently been studied by a number of groups using different types of polymer models. Linear polyelectrolytes with Coulomb interactions have been studied by Reed and Reed[5] and a polyelectrolyte with attractive interactions on a cubic lattice has been simulated by Sassi *et al.*[6] These two simulations have been performed in the grand canonical ensemble with a fixed bulk chemical potential and a varying degree of ionization on the chain. Simulations in the canonical ensemble with a partial but fixed degree of ionization have also appeared in the literature.[7–11] The studies of titrating polymers have been limited to rather short chains, of the order of 100, while nontitrating polyelectrolytes of up to 2–400 monomers have been studied by a number of groups.[11–13] Only recently have longer chains been treated.[14,15]

Most simulation algorithms are very inefficient for polymers and single move algorithms have very poor convergence properties for global properties like the average end-to-end separation. Improved convergence characteristics may be obtained with the reptation method or by the ensemble growth method.[10,12] (A thorough review of Monte Carlo

[a]fk2mul@dix.fkem2.lth.se
[b]fk2boj@grosz.fkem2.lth.se
[c]bs@thep.lu.se
[d]carsten@thep.lu.se

 0021-9606/96/104(8)/3048/10/$10.00

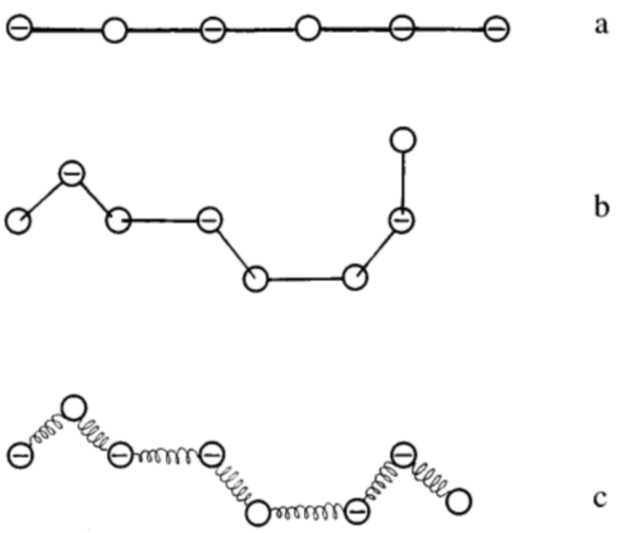

FIG. 1. Schematic picture of the polyelectrolyte models. (a) Model 1 consists of a rigid rod with fixed bond lengths between monomers. (b) Model 2 contains rigid bonds, but has a complete angular freedom. (c) Model 3 is a flexible chain with monomers connected by harmonic bonds.

techniques for polymers has recently been published by Kremer and Binder.[16]) In order to really improve the convergence and extend the simulations to chains with several thousand monomers, one has to use global move algorithms. One such algorithm is the pivot method,[17,18] while a different approach has recently been proposed by Irbäck,[19] in which the Gaussian chain is used to identify slow collective modes. We have found that the pivot algorithm and the Irbäck method are of comparable efficiency and both scale approximately like N^3 for an extended polymer chain. In this work we have used the pivot method, allowing simulation of chains with several thousand monomers.

II. MODELS

The polyelectrolyte is regarded as an infinitely diluted polyacid in a salt-free solution. The monomers form a linear chain where each monomer represents a titrating site that can be either protonated or deprotonated, i.e., be uncharged or carry one unit of negative charge. Three different models have been considered: Model 1 is a strictly linear polyelectrolyte with rigid bonds (a rigid rod). In Model 2 the chain is allowed to bend, while monomer–monomer bonds are still rigid, and in Model 3 this constraint is relaxed and the monomers are joined by harmonic bonds[20]—the three models are schematically shown in Fig. 1. The harmonic bonds correspond to an approximately Gaussian distribution of bond lengths and can be viewed as an averaging over the conformational freedom of the covalent structure that implicitly joins the titrating sites.

The solvent is treated as a dielectric continuum of a given permittivity equal to that of water at room temperature and the effect of the solvent will only enter into the Hamiltonian as a dielectric screening of electrostatic interactions. Thus charged monomers interact via a Coulomb potential, E_C, which for the flexible bond model (Model 3) is augmented with a Gaussian term, E_G, leading to a total interaction energy

$$E=E_G+E_C=\frac{k}{2}\sum_{i\neq N} r_{i,i+1}^2+\frac{e^2}{4\pi\epsilon_r\epsilon_0}\sum_i\sum_{j>i}\frac{Z_iZ_j}{r_{i,j}}, \qquad (1)$$

where N is the number of monomers, $r_{i,j}$ is the distance between monomer i and j, e is the electronic charge, ϵ_r is the dielectric constant of the solution (78.3 in all simulations), ϵ_0 is the permittivity of vacuum, and Z_i the amount of charge on monomer i (either 0 or -1). The force constant, k, is given implicitly through the input parameter $r_0=(e^2/4\pi\epsilon_r\epsilon_0 k)^{1/3}$, which is the equilibrium distance for a fully charged dimer.

In most of the simulations reported here uncharged, nonbonded monomers do not interact, i.e., there are no angular or hard core constraints. In Models 2 and 3 such monomers may therefor occupy the same position. In a few simulations with rigid bonds we have introduced hard cores on all monomers with a hard sphere diameter of 3 Å, i.e., two monomers may not come closer than this distance.

III. MONTE CARLO SIMULATIONS

The Monte Carlo (MC) simulations were performed with the traditional Metropolis algorithm[21] in a semigrand canonical ensemble. One polyelectrolyte chain was simulated with the charges/protons moving between the monomers and an implicit bulk of fixed chemical potential. When a proton move is attempted, a monomer is picked at random and the charge state of the monomer is switched. The associated (free) energy change, ΔE, which determines if the move is to be accepted or rejected according to the Metropolis scheme, is the sum of the change of intramolecular Coulomb energy, ΔE_C, and a term that corresponds to the change in free energy for the acid-base reaction of an isolated monomer

$$\Delta E=\Delta E_C\pm k_BT\ln 10(pH-pK_0), \qquad (2)$$

where k_B is Boltzmann's constant, T is the temperature, pH is the pH of the bulk, and pK_0 is the intrinsic pK_a of a monomer. The difference $pH-pK_0$ is an input parameter of the program. The plus sign is used when the monomer is to be protonated and the minus sign when it is to be deprotonated. In a single MC step a proton is only moved from the chain to the bulk or *vice versa*. Adding a step where a proton moves within the polymer does not affect the averages but increases the calculation time.

The sampling of chain conformations is made highly efficient, compared to traditional Monte Carlo moves, by using a pivot algorithm, which allows chain lengths of more than 2000 monomers. The pivot algorithm was first described by Lal,[17] and its efficiency for self-avoiding walks have been thoroughly discussed by Madras and Sokal.[18] Despite its excellent properties the pivot algorithm is still just beginning to gain wider recognition. Recently it has been used by Bishop *et al.* for simulations of uncharged polymers,[22] and by ourselves and others for polyelectrolytes.[14,15,23,24]

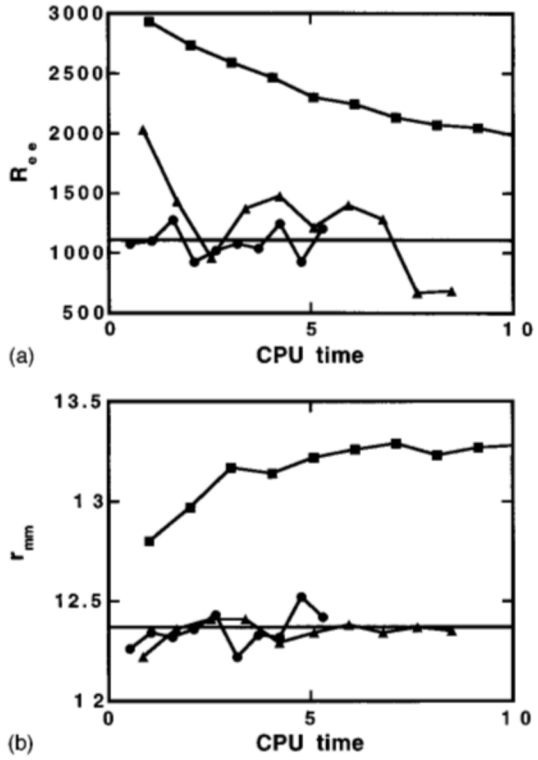

FIG. 2. The evolution in terms of CPU time of (a) the end-to-end distance and (b) the monomer–monomer separation during simulations of Model 3 with a screened Coulomb potential using different move algorithms: traditional single move (squares), translational pivot (triangles), and pivot with translations and rotations (circles). The unit of length is Å.

In Model 3 a traditional move is to attempt a translation of only one monomer at a time. The number of interactions that has to be calculated is of the order N for a highly charged chain and a large number of attempts per monomer are needed to generate independent chain conformations. Similarly, in the pivot algorithm each monomer i (except the first one) is translated in turn but together with the remaining subchain (monomers $i+1$ to N). Furthermore, the last part of the polymer is then rotated as a rigid body around one of the coordinate axes with monomer i as origin. The number of interactions calculated in one step is of the order N^2, but independent conformations are obtained after only a few attempted moves, on the order of one per monomer or N in total. The net effect is a greatly reduced simulation time for a given degree of precision and a computational cost that grows approximately as N^3.

Just to give an example, Fig. 2(a) shows how the end-to-end separation develops during the course of a simulation. The traditional "single move" algorithm is clearly inferior to any of the two pivot algorithms and the former becomes virtually impossible to use for chains containing more than a few hundred monomers. One expects the pivot algorithm to have its maximal efficiency for unscreened and extended chains, but Fig. 2 demonstrates its high efficiency even for screened chains with less elongated structure. The pivot algorithm provides an effective sampling of not only global properties like R_{ee}, but also for more local ones like the average monomer-monomer separation [see Fig. 2(b)].

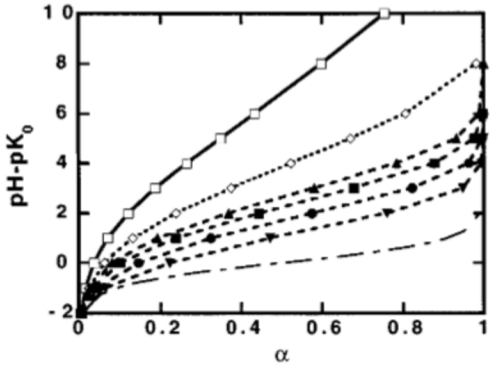

FIG. 3. Titration curves for the rigid bond case (Model 2). The curves (with symbols) show from top to bottom: $a=3$ Å (solid line, open squares) and $a=6$ Å (dotted line, open diamonds) for $N=320$ and $a=12$ Å (dashed lines, filled symbols) for $N=1000$ (triangles pointing up), 320 (squares), 80 (circles) and 20 (triangles pointing down). Also shown is the curve for isolated monomers, $pH-pK_0=\lg[\alpha/(1-\alpha)]$ (dot–dashed curve without symbols).

In the simulations presented here a change in conformation is attempted once in every 20 steps. In the remaining steps, a change in the charge state is attempted. The total number of steps is between 10^7 and 10^8. Every run is preceded by an equilibration of 10^5–10^6 steps, where a change in conformation is attempted every other step, starting from a straight line with a charge on every other monomer. The simulations are faster at low $pH-pK_0$ since fewer monomers are charged, and thus the number of interactions that have to be calculated is smaller.

IV. RESULTS AND DISCUSSION

The degree of dissociation, α, increases with pH, which means that the amount of charge on the polyelectrolyte increases and further dissociation becomes more difficult. This can be measured, for example, by potentiometric titration, as an increasing apparent dissociation constant,

$$pK=pH-\lg\frac{\alpha}{1-\alpha}. \tag{3}$$

This is also the expression for the intrinsic dissociation constant, pK_0, in the case of isolated monomers (dilute monoacid). The difference between the apparent and intrinsic dissociation constants, $\Delta pK=pK-pK_0$, is related to the excess free energy, F, due to the interaction between monomers through

$$\Delta pK=\frac{1}{Nk_BT\ln 10}\frac{\partial F}{\partial\alpha}. \tag{4}$$

Figure 3 shows a set of typical titration curves for Model 2 along with the "ideal" titration curve, i.e., the curve for isolated monomers ($pK=pK_0=$constant). ΔpK is the difference between a titration curve and the ideal curve, though in a simulation the value is obtained directly using Eq. (3) since pK_0 is an undetermined reference. Note that experimentally α is varied (strong base added) and the pH is measured. In

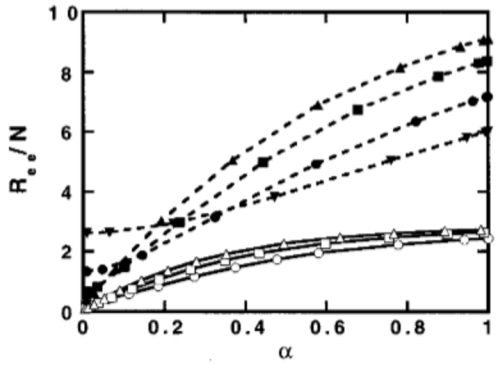

FIG. 4. The root-mean-square end-to-end separation R_{ee}/N as a function of α for Model 2. Line types and symbols are the same as in Fig. 3 with open symbols (and solid lines) used for $a=3$ Å and filled symbols (and dashed lines) for $a=12$ Å.

the simulations it is the other way around, α is measured for different values of $pH-pK_0$. Decreasing the monomer–monomer separation from 12 to 3 Å in a chain with 320 monomers leads to a large increase in ΔpK of more than eight pK units, which would be difficult to observe experimentally. In a real experiment the presence of counterions and added salt would screen the electrostatic interactions and lead to a more modest increase in ΔpK.[25] The curves show that an increased chain length will also affect ΔpK, but to a much lesser extent than the monomer–monomer separation. For example, the difference between a fully ionized 20-mer and a 1000-mer is only two pK units.

Figure 4 describes the expansion of the polymer chain upon ionization (Model 2) in terms of the root-mean-square end-to-end separation, R_{ee}

$$R_{ee}^2=\langle r_{1,N}^2\rangle. \tag{5}$$

The fact that the curves for different N cross at some point is only a reflection of the transition between a Gaussian chain and an electrostatically extended one. An interesting observation is that R_{ee}/N is an increasing function of N and still increases at $\alpha=1$ for a 1000-mer with a bond length $a=12$ Å. For a polymer with rigid bonds (Model 2) R_{ee} has to increase linearly with N for sufficiently large N. This limiting behavior is seen for highly charged chains with small monomer–monomer separation, i.e., $a=3$ Å.

The purpose of this work is to try to rationalize the exact MC results on the basis of simpler approximate theories, thereby hoping to obtain a better understanding of the physical mechanisms governing the titration behavior of a polyelectrolyte. For this purpose we will, as a first step, compare the MC simulations for flexible chains to the mean field solution for a rigid rod, which can be solved analytically. As a second comparison, we will use different variational approaches to the uniformly charged chain. We will focus the comparisons on R_{ee} and the apparent dissociation constant ΔpK as well as the electrostatic energy, $\langle E_C\rangle$.

A. The rigid rod

The acidic behavior of the rigid rod can be described with a mean field treatment. If each monomer is regarded to carry an effective charge equal to the degree of dissociation, α, then the Coulomb energy per monomer may be approximated as

$$\tilde{E}=\frac{\langle E_C\rangle}{Nk_BT}=\frac{l_B\alpha^2}{N}\sum_{k=1}^{N-1}(N-k)\,\frac{1}{ka}=\frac{l_B}{a}\,\alpha^2\sum_{k=2}^{N}\frac{1}{k}, \tag{6}$$

where $l_B=(e^2)/(4\pi\epsilon_r\epsilon_0k_BT)$ is the Bjerrum length (ca. 7.16 Å in all simulations, which were performed at 298 K) and a is the bond length. The last sum is approximately $\ln N-0.42$ for $N>80$, which is most easily seen by direct calculation. For $N=80$, 320, and 2000 the correction to the logarithm is -0.4165, -0.4212, and -0.4225, respectively. As $N\to\infty$ the correction tends to $\gamma-1$, where γ is the Euler–Mascheroni constant ($\gamma=0.577\,215\,66\cdots$).[26] The approximate energy is

$$\tilde{E}_{\mathrm{MF}}=\frac{l_B}{a}\,\alpha^2(\ln N-0.42). \tag{7}$$

In the mean field treatment of the rigid rod there is no entropy and the Coulomb energy is also the excess free energy. Combining Eqs. (4) and (7) and introducing $\tilde{F}=(F_C)/(Nk_BT)$ gives

$$\Delta pK_{\mathrm{MF}}=\frac{1}{\ln 10}\frac{\partial\tilde{F}_{\mathrm{MF}}}{\partial\alpha}=\frac{1}{\ln 10}\frac{\partial\tilde{E}_{\mathrm{MF}}}{\partial\alpha}$$

$$=\frac{2}{\ln 10}\frac{l_B}{a}\,\alpha(\ln N-0.42). \tag{8}$$

Figure 5(a) shows the difference in Coulomb energy per monomer obtained from simulation with Model 1 and from Eq. (7) as a function of α. The agreement is good and even with a rather low value of $a=3$ Å, the error is but a few tenths of k_BT, which in relative terms corresponds to 10%–20%. With a more reasonable value of $a=12$ Å the largest error is less than 0.1 k_BT and in relative terms less than a few percent. The mean field approximation is trivially exact in the two extremes and the largest error is found around $\alpha=0.5$. It is interesting to note that the error/monomer is independent of N, which means that the major part of the correlation error is local in nature.

The mean field prediction for ΔpK is investigated in Fig. 5(b) for different bond lengths and numbers of monomers. The agreement is very good and for $a=12$ Å the mean field is essentially exact, while the largest error equal to 0.3 pK units is found for $a=3$ Å. The mean field error in ΔpK is obviously also independent of N, at least for chains with more than 20 monomers.

The mean field approximation, Eq. (6), can be decomposed into two parts: (i) the neglect of two-particle and higher order correlations by assuming that the actual charge on site i is independent of the charge on site $j\neq i$, (ii) the neglect of one-particle correlations, i.e., the average charge on site i $\langle\alpha_i\rangle=\alpha$ is constant and independent of i. Figure 6 shows that α_i is a rather uniform function of i for small α. With increasing degree of ionization there is, however, an

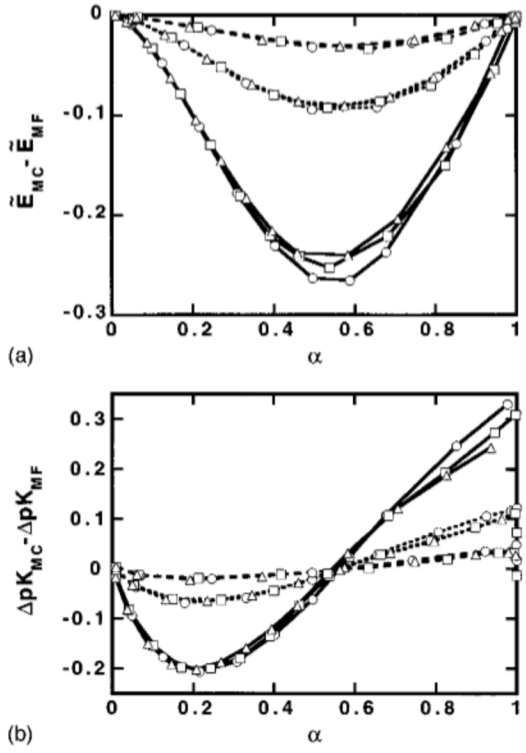

FIG. 5. Comparisons between simulation results and the mean field approximation [Eqs. (7) and (8)] for rigid rods (Model 1) with bond lengths, a, of 3 Å (solid lines), 6 Å (dotted lines), and 12 Å (dashed lines) and numbers of monomers, N, of 80 (circles), 320 (squares), and 1000 (triangles). (a) The difference in Coulomb energy per monomer as a function of α. (b) The difference in ΔpK as a function of α. As in (a), the largest difference is seen for $a=3$ Å and the smallest for $a=12$ Å.

accumulation of charge towards the ends, which again disappears when $\alpha\approx 1$, i.e., when the chain becomes fully charged.

Thus we conclude that the mean field solution to the rigid rod model of a titrating polyelectrolyte is quite accurate. A rough estimate of the one-particle correlation error could probably be made by allowing the charges to accumulate at the ends. The question that arise is of course how

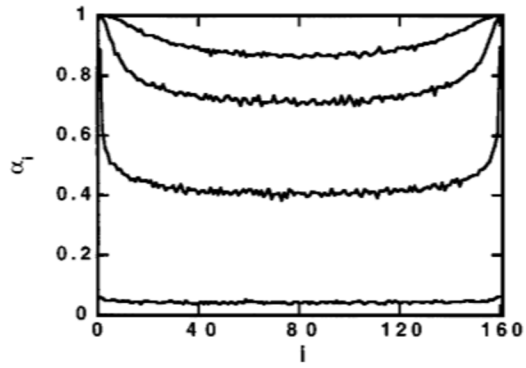

FIG. 6. The degree of dissociation as a function of position along rigid rods with $N=160$ and $a=3$ Å at $pH-pK_0=10$, 8, 4, and -1 (top to bottom). The overall degrees of dissociation, α, are 0.907, 0.760, 0.437, and 0.044, respectively.

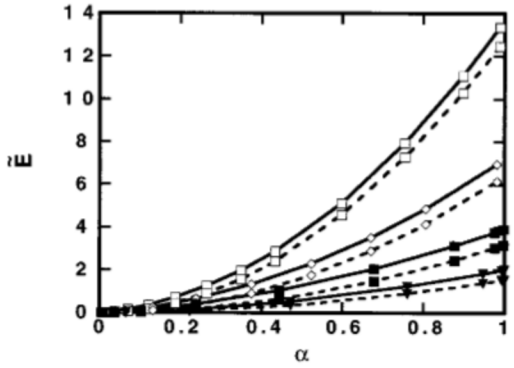

FIG. 7. Coulomb energy per monomer from simulations of flexible chains (Model 2) (solid lines) and the mean field results [Eq. (7)] for the corresponding rigid rods (dashed lines). The symbols are the same as in Fig. 3.

realistic the rigid rod model is for a real flexible polyelectrolyte. This problem will be further analyzed below.

B. The flexible chain as an effective rigid rod

There is no angular potential in Models 2 and 3 and the angle between two successive bonds can vary between 0° and 180° only hindered by electrostatic interactions. For Model 2, which we will concentrate on in this section, the flexibility will increase the electrostatic repulsion between charged monomers as compared to a rigid rod and as a consequence ΔpK will also increase. This difference between the rigid rod and a flexible chain will vary with chain length, bond length and degree of ionization and it will decrease as the Coulomb repulsion increases.

Figure 7 shows that the mean field rigid rod provides a rather good approximation to the Coulomb energy of a flexible chain. The mean field, in contrast to the previous case, now underestimates the electrostatic interactions, since it does not account for chain folding. The neglect of correlation in the mean field approximation leads to an overestimate of the Coulomb energy, while the use of a rigid rod underestimates the interactions. These two errors partly compensate and the comparison in Fig. 7 comes out quite favorably, with the relative difference decreasing with α.

The same can be said for the mean field result for ΔpK. It has been obtained directly from the mean field energy and the results indicate that the electrostatic energy gives the major contribution to ΔpK and that the contribution from the conformational entropy is small by comparison. This is confirmed by Fig. 8, which compares simulated ΔpK values to their energetic contributions, obtained by numerical derivation of the energy with respect to α [cf. Eq. (8)]. The mean field result for ΔpK is compared to simulation results in Fig. 9. In particular Fig. 9(b) shows that the rigid rod approximation describes the behavior very well in terms of bond lengths and number of monomers. At large α the error is almost constant. The deviations are largest at low values of α, which is further emphasized by the relative difference shown in Fig. 9(c). (The corresponding curves for the relative difference in energy are virtually identical.) This is to be expected since a low degree of ionization allows the chain to

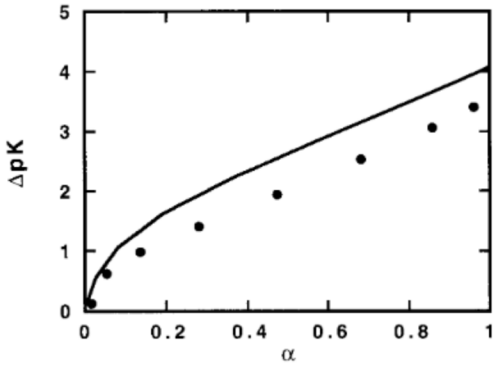

FIG. 8. ΔpK (solid line) and the energetic contribution (circles) obtained from numerical derivation of the Coulomb energy with respect to α. The data comes from simulations of a 1000-mer with a bond length of 12 Å (Model 2).

contract and partly fold back on itself, increasing the local monomer density and thus the electrostatic interactions and ΔpK. This is in contrast to the rigid rod where the monomer concentration is constant and the interactions are ordered in the sense that monomers far apart in sequence also are far apart in space. As the expansion increases, however, the flexible chain will become more ordered and the rigid rod approximation better.

Anything that will increase the stiffness of the chain will improve the agreement. An increased coupling, which may be expressed as $\alpha \ln N/a$, will have this effect, i.e., besides a larger degree of ionization, more monomers and shorter bonds will make the chain more rodlike. The addition of a short range potential in terms of a hard core on each titrating group will also help to expand the chain. In Fig. 9(a) it is shown how hard-sphere contacts remove much of the deviations at low α. At large degrees of ionization the electrostatic energy takes over and the hard cores have no effect. Any angular potential restricting the chain conformation will of course work in the same direction and the discrepancies seen in Fig. 9 are in this respect upper limits.

For chains with flexible bonds (Model 3) the comparisons are qualitatively the same, provided that the monomer–monomer separation a is replaced by the average monomer–monomer separation, r_{mm}, defined as

$$r_{\mathrm{mm}}^2 = \frac{\Sigma_i^{N-1}\langle r_{i,i+1}^2\rangle}{N-1}. \tag{9}$$

C. Variational ansatz

In a Flory type ansatz[27,28] we can try to approximate the excess free energy as a sum of an electrostatic energy and an elastic free energy or entropy. Inspired by the mean field results for the rigid rod we here write the electrostatic energy as that for a rigid rod, Eq. (7). The entropy is assumed to be that of an expanded freely jointed chain,

$$\tilde{F} = \frac{l_B \alpha^2 N \ln N}{R} + \frac{3}{2}\left(\frac{R}{Na}\right)^2, \tag{10}$$

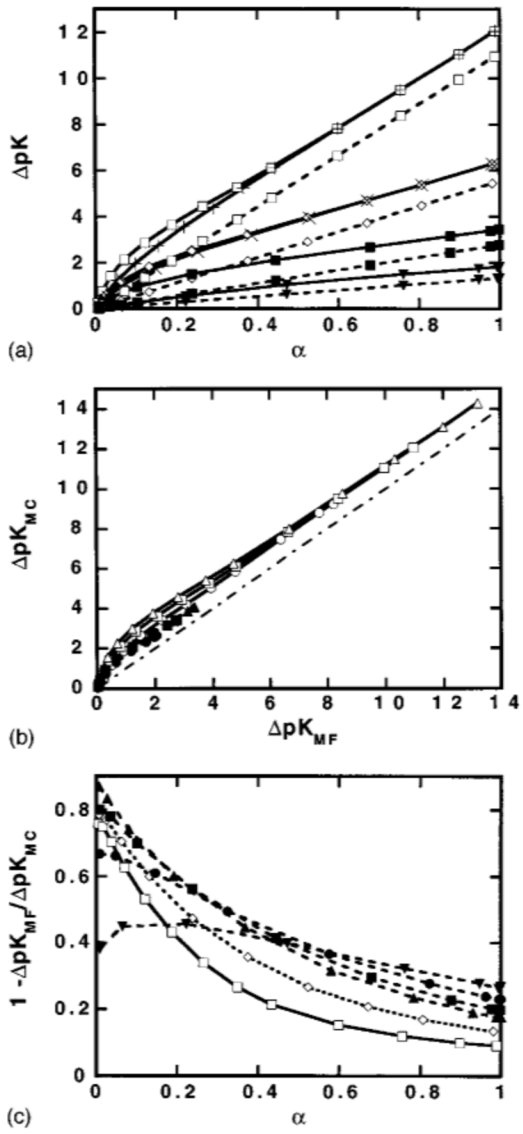

FIG. 9. Comparisons of ΔpK from simulations of flexible chains (Model 2) and the mean field results [Eq. (8)] for the corresponding rigid rods. (a) ΔpK as a function of α. Solid lines are simulated data, while dashed lines represent the rigid rod results. In addition to the chains with pointlike monomers (see below) two 320-mers with hard-sphere monomers (diameter 3 Å) are displayed for $a=3$ Å (plus signs) and $a=6$ Å (crosses). (b) Monte Carlo results against the corresponding mean field approximations. The dot–dashed curve corresponds to $y=x$. (c) The relative difference as a function of α. With the exception of the line rules in (a), chains with pointlike monomers and rigid bonds are depicted in the following way: For $a=3$ Å (solid lines, open symbols) and $a=12$ Å (dashed lines, filled symbols) triangles pointing down, circles, squares, and triangles pointing up denote $N=20$, 80, 320, and 1000, respectively. A 320-mer with $a=6$ Å is represented by a dotted line and open diamonds.

where we will identify R as the end-to-end separation. It is clear that this entropy approximation is only justified for a polymer with rigid bonds if the deviation from the Gaussian chain is "small," i.e., R_{ee}/Na should not be larger than approximately 0.6–0.7.[29] We now seek a variational solution by minimizing the free energy with respect to R,

$$R = \frac{1}{3^{1/3}}(l_B a^2)^{1/3}\alpha^{2/3} N[\ln N]^{1/3}. \tag{11}$$

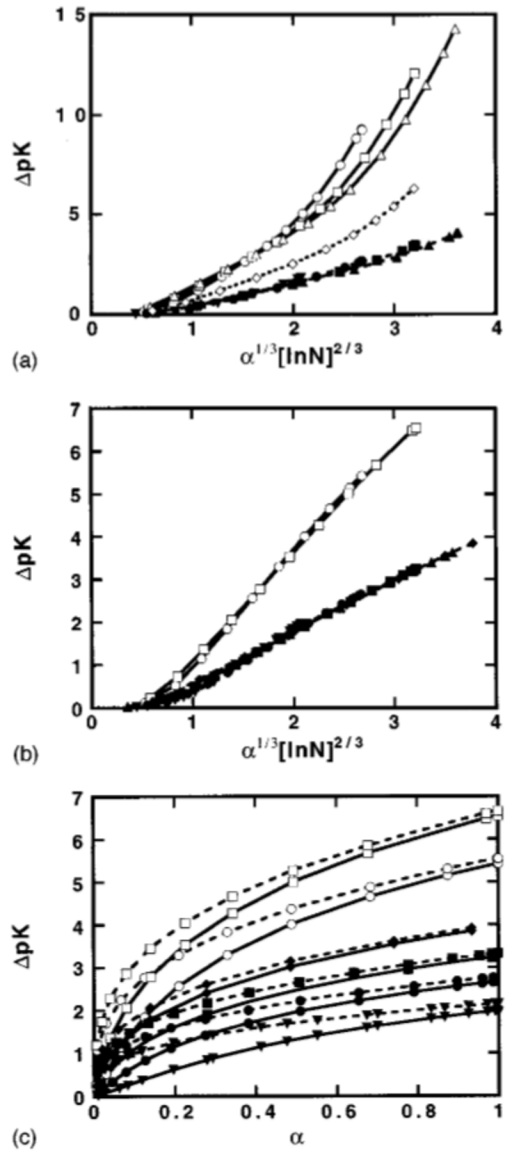

FIG. 10. ΔpK as a function of $\alpha^{1/3}[\ln N]^{2/3}$ (a) for Model 2 and (b) for Model 3. (c) ΔpK from simulations of Model 3 (solid lines) compared to the variational results of Eq. (22) (dashed lines). The line types and symbols in (a) are the same as in Fig. 9(b). In (b) and (c) the following system for flexible bonds is used: The bond parameter r_0 is represented by open symbols for r_0=3 Å and by filled symbols for r_0=6 Å. Triangles pointing down, circles, squares, triangles pointing up and diamonds denote N=20, 80, 320, 1000, and 2000, respectively. In (b) solid and dashed lines are merely additional identifiers for r_0=3 and 6 Å, while in (c) solid lines mark simulated data and dashed lines the variational results as stated.

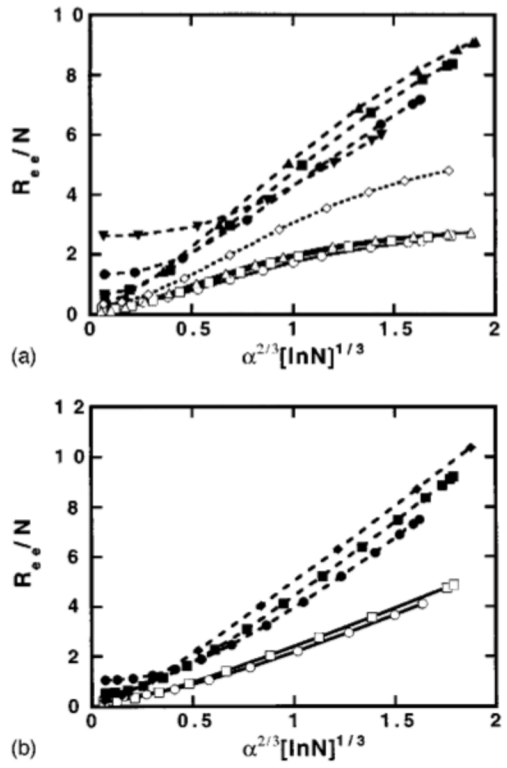

FIG. 11. The root-mean-square end-to-end separation R_{ee}/N in Å as a function of $\alpha^{2/3}[\ln N]^{1/3}$ (a) for Model 2 and (b) for Model 3. Line types and symbols are the same as in Figs. 9(b) and 10(b), respectively.

To obtain ΔpK we need to differentiate the free energy with respect to α and with Eq. (11) we get

$$\Delta pK = \frac{2\cdot 3^{1/3}}{\ln 10}\left(\frac{l_B}{a}\right)^{2/3}\alpha^{1/3}[\ln N]^{2/3}. \tag{12}$$

Thus a comparison between Eqs. (8) and (12) shows that the functional behavior of the two approximations, the rigid rod and the Flory ansatz, are quite different as regards both α, N, l_B, and a. Figure 10(a) shows that ΔpK for a flexible polymer with rigid bonds is not a linear function of $\alpha^{1/3}[\ln N]^{2/3}$, which is predicted by Eq. (12). At moderate coupling the relation between α and $\ln N$ seems to give a good description of the scaling behavior, but the lines are curved, which indicates that the exponents are not optimal. A numerical investigation gives an α exponent of 0.5–0.6 at intermediate coupling, although it varies with bond length and degree of ionization. At strong coupling the scaling relation breaks down completely.

The breakdown originates in the entropic term since the quadratic R dependence allows the chain to grow indefinitely. This term can be derived by considering a force, τ, stretching a freely jointed chain.[29,30] In this approach the end-to-end distance can be obtained directly in terms of a Langevin function,

$$R = Na(\coth(t) - 1/t). \tag{13}$$

where $t=\tau a/k_BT$. The harmonic entropy term is obtained in the limit of low t, i.e., $\tau a \ll k_BT$. Of course, Eq. (13) can be used directly [$\coth(t)\approx t/3+1/t$ for small t]. It gives the same end-to-end distance as the Flory approach, Eq. (11), if τ is identified with the electrostatic force $-(\partial E_C)/(\partial R)$ calculated from the first term in Eq. (10).

In the limit of large t ($\tau a \gg k_BT$), the force can be approximated by $t=(1-R/Na)^{-1}$,[30] which translates to

$$-\frac{l_B\alpha^2 N\ln N}{R^2}+\frac{1}{(Na-R)}=0. \tag{14}$$

This force balance corresponds to $\partial\tilde{F}/\partial R$ in the Flory approach. Equation (14) is nothing but a second order equation with the positive root

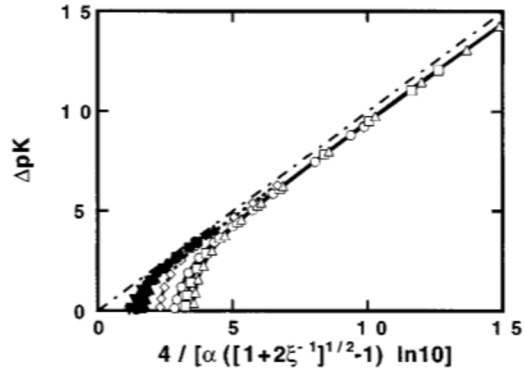

FIG. 12. Simulated ΔpK compared to the strong coupling approximation of Eq. (14). Line types and symbols are the same as in Fig. 9(b).

$$R = Na\xi(\sqrt{1+2\xi^{-1}}-1), \tag{15}$$

where we have introduced the coupling parameter

$$\xi \equiv \frac{1}{2}\frac{l_B}{a}\alpha^2 \ln N. \tag{16}$$

Carrying the analysis through for ΔpK we get

$$\Delta pK = \frac{4}{\alpha(\sqrt{1+2\xi^{-1}}-1)\ln 10}. \tag{17}$$

Note that when ξ is very large, R equals Na and ΔpK is the same as for the rigid rod, Eq. (8), i.e., the end-to-end distance is asymptotically correct and so is ΔpK in the mean field picture. Figures 12 and 13 confirm that this is indeed an improvement in the strong coupling regime compared to the original Flory result [Figs. 10(a) and 11(a)] for rigid bonds. The agreement in Fig. 12 can actually be made quantitative by shifting the curves to the left. To be specific, the linear parts of the curves will fall onto the line $y=x$, if the empirical correction $(0.8/\ln 10)\sqrt{l_B/a}$ is subtracted from the right-hand side of Eq. (17).

If we turn our attention to chains with flexible bonds, we get another picture. They can expand by adopting more extended conformations in the same way as the rigid bond chains, but they can also expand by stretching the bonds between monomers. The latter expansion is of course unlimited and only hindered by an increasing harmonic energy, which allows a surviving $\ln N$ dependence. Indeed, Figs. 10(b) and 11(b), indicate that Model 3 follows the general scaling behaviour predicted by Eqs. (12) and (11). These expressions were derived considering the conformational entropy of a rigid bond chain, but we can get similar expressions from a slightly different approach. Let us consider a chain with flexible bonds at strong coupling: In this limit the chain has already approached a collinear structure and the conformational entropy of the chain is negligible. The individual monomer–monomer bonds can still expand and the excess free energy can be expressed as,

$$\tilde{F} = \frac{l_B\alpha^2 N}{R}\ln N + \frac{\tilde{k}}{2}\left(\frac{R}{N}\right)^2, \tag{18}$$

where $\tilde{k}$ is the force constant of the bonds rescaled by k_BT, $\tilde{k}=k/k_BT=l_B/r_0^3$ [see Eq. (1)]. Equation (18) is functionally analogous to the previous free energy expression, Eq. (10), but the quadratic term now comes from the exact Hamiltonian, Eq. (1), and the variational ansatz that the chain is a straight rod with an effective bond length R/N. Of course, a similar end-to-end separation is found as in Eq. (11) by minimizing the free energy,

$$R = r_0\alpha^{2/3}N[\ln N]^{1/3} \tag{19}$$

but it is now a valid limiting expression. The exponent for the logarithmic term, $\ln N$, should be 1/3 according to Eq. (19), but the curves i Fig. 11(b) indicate a slightly stronger N dependence, 0.6–0.7. We believe that this is an intermediate phenomenon, which is coupled to the conformational freedom, i.e., a rigid bond behavior (cf. the next subsection). For sufficiently long and strongly coupled chains R_{ee}/N will scale as $[\ln N]^{1/3}$. The α exponent is also slightly larger than expected, about 0.85 compared to 2/3. The slope of the curves is predicted to be equal to r_0, which is indeed found to be the case in Fig. 11(b).

Equation (19) can be viewed as N times the component of a bond vector along the end-to-end vector. In order to obtain the full monomer–monomer separation, fluctuations in other directions have to be considered. This can be done through the use of the virial identity[15]

$$2\langle E_G\rangle - \langle E_C\rangle = 3(N-1)k_BT \tag{20}$$

which leads to

$$r_{\mathrm{mm}}^2 = \left(\frac{R_v}{N}\right)^2 + \frac{3r_0^3}{l_B} = r_0^2\alpha^{4/3}[\ln N]^{2/3} + \frac{3r_0^3}{l_B}. \tag{21}$$

This expression is virtually exact for all coupling strengths, due to the use of the virial identity, which is obeyed at all times. The second term, $3r_0^3/l_B$, is the mean-square monomer–monomer separation, r_{mm}^2, in the absence of charge.

Based on Eqs. (18) and (19) the shift in the apparent dissociation constant becomes,

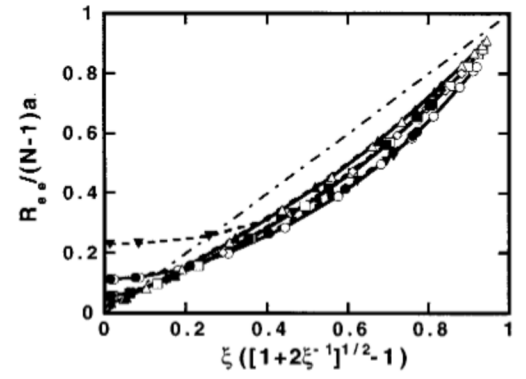

FIG. 13. Simulated end-to-end distance divided by the contour length compared to the strong coupling approximation of Eq. (13). Line types and symbols are the same as in Fig. 9(b).

$$\Delta pK = \frac{2}{\ln 10}\frac{l_B}{r_0}\,\alpha^{1/3}[\ln N]^{2/3}. \tag{22}$$

Figure 10(b) shows that the simulated shifts for a chain with flexible bonds, in contrast to rigid bonds, vary approximately linearly with $\alpha^{1/3}(\ln N)^{2/3}$ in the limit of strong coupling. At decreasing coupling, the exponent of the product increases. It is also found that ΔpK multiplied by r_0/l_B is nearly independent of r_0. Equation (22) not only gives approximately the correct asymptotic behavior, but it also provides quite good numerical estimates for ΔpK as can be seen in Fig. 10(c). There is a significant discrepancy at low α, but it gives an accurate estimate at intermediate and high α. Thus we conclude that the variational approach gives a correct limiting behavior for ΔpK for a chain with flexible bonds.

We have here tried to describe the simulation results with the help of a very simple variational approach. A more full-blown variational treatment is described and applied elsewhere.[15,31]

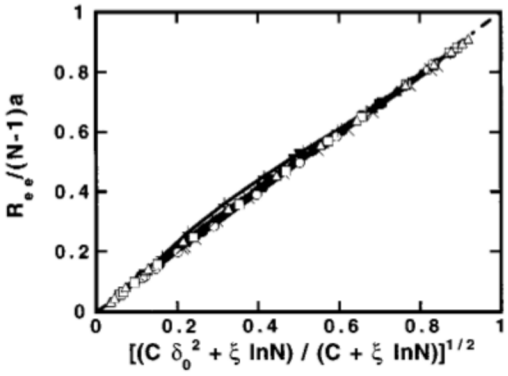

FIG. 14. The end-to-end distance divided by the contour length vs the empirical trial expression of Eq. (23) with $C=10$. Results are shown for Model 2 with bond lengths 3 Å (solid lines, open symbols) and 12 Å (dashed lines, filled symbols). The numbers of monomers are 20 (triangles pointing down), 80 (circles), 320 (squares), and 1000 (triangles pointing up). An 80-mer (crosses) and a 320-mer (plus signs) with hard-sphere monomers (diameter 3 Å) and a bond length of 3 Å are also included (solid lines). The dot–dashed line hiding under the other curves corresponds to $y=x$.

D. Empirical end-to-end expression

So far we have used different mean field expressions to rationalize the numerical data and to find approximate relations. One can also try to use the simulated numbers in a more empirical approach searching for universal behavior of different chain properties. By investigating the results we find that the the end-to-end distance divided by the contour length, $R_{ee}/(N-1)a$, is a function of $\alpha \ln N/\sqrt{a}$. An approximate expression may be suggested by considering the limits of no coupling and very strong coupling,

$$\delta \equiv \frac{R_{ee}}{(N-1)a} \approx \sqrt{\frac{C\,\delta_0^2 + \xi\,\ln N}{C + \xi\,\ln N}}, \tag{23}$$

with ξ defined as before. δ_0 is the value of δ at $\alpha=0$ (for pointlike monomers $\delta_0=(N-1)^{-1/2}$) and C is a constant. If the trial expression is fitted to the simulation data, the value of C is not constant, but nearly so. In the case of rigid bonds (Model 2) the value of the pseudo constant lies within the range 8–12 when $\alpha>0.3$ for the chains considered here. In Fig. 14 the left-hand side of Eq. (23) is plotted against the right-hand side with $C=10$. The agreement is excellent when the monomers are pointlike. The curves for hard-sphere monomers show deviations from a quantitative agreement at low and intermediate coupling. This indicates that the correction term $C\delta_0^2$, which forces the expression to be exact at $\alpha=0$, i.e., at $\xi=0$ (δ_0 was obtained directly from simulations in the hard-core case), does not give a good description of the behavior at low coupling. In fact, a small deviation can also be seen for the 1000-mer with pointlike monomers and this seems to be the trend when the chain length increases. When the coupling is strong, the short-range potential loses significance and all the chains display the same behavior and the curves coincide. In other words, the trial expression, Eq. (23), has the marks of asymptotic behavior in the strong coupling regime when compared to simulations. This is not the case at the other end of the scale, but the $\alpha=0$ correction still makes for a good approximation. The major point, however, is that $\xi \ln N = (l_B/2a)(\alpha \ln N)^2$ is a good parameter.

Chains with flexible bonds behave similarly when the rigid bond length a is replaced by the root-mean-square monomer–monomer separation r_{mm}.

V. CONCLUSIONS

The simulation of charged polymers is most efficiently performed with the so-called pivot algorithm and the computational effort increases approximately as the number of monomers to the third power.

The mean field solution for a rigid rod provides a qualitatively correct description of the titration behavior even for a flexible chain at intermediate to strong coupling. The approximation neglects any correlation between ionizing sites as well as any conformational dependence. These two factors cancel to some extent. Furthermore, ΔpK is dominated by the energetic term, which also contributes to the relative success. The mean field rigid rod approach is primarily applicable to chains with rigid bonds, but can be used for flexible bonds if the average monomer–monomer separation is known.

The traditional Flory approach based on a freely jointed chain gives a qualitatively correct picture only at intermediate coupling strengths. It breaks down for rigid bonds at strong coupling where it for example predicts that R_{ee} increases more than linearly with N. The reason is that the entropy approximation becomes deficient. The correct scaling behavior can be regained, however, by replacing the low coupling approximation with a corresponding strong coupling one.

Flexible chain with harmonic bonds seems to be better described by the scaling predictions of the Flory approach. This is due to the microscopic flexibility of the bonds rather than the macroscopic, conformational one, which is the basis of the freely jointed chain approach. It is therefore prefer-